

Invariant Causal Knowledge Distillation in Neural Networks

Nikolaos Giakoumoglou
Imperial College London
London, UK, SW7 2AZ

n.giakoumoglou23@imperial.ac.uk

Tania Stathaki
Imperial College London
London, UK, SW7 2AZ

t.stathaki@imperial.ac.uk

Abstract

Knowledge distillation (KD) involves transferring the knowledge from one neural network to another, often from a larger, well-trained model (teacher) to a smaller, more efficient model (student). Traditional KD methods minimize the Kullback-Leibler (KL) divergence between the probabilistic outputs of the teacher and student networks. However, this approach often overlooks crucial structural knowledge embedded within the teacher’s network. In this paper, we introduce Invariant Consistency Distillation (ICD), a novel methodology designed to enhance KD by ensuring that the student model’s representations are both discriminative and invariant with respect to the teacher’s outputs. Our approach is based on causal inference principles and combines contrastive learning with an explicit invariance penalty, capturing significantly more information from the teacher’s representation. ICD uses an efficient, parameter-free approach for flexible teacher-student alignment. We provide a theoretical foundation for ICD and demonstrate its effectiveness through extensive experiments. Our results on CIFAR-100 and ImageNet ILSVRC-2012 show that ICD outperforms traditional KD techniques and surpasses state-of-the-art methods. In some cases, the student model even exceeds the teacher model in terms of accuracy. Furthermore, we successfully apply our method to other datasets, such as Tiny ImageNet and STL-10, demonstrating superior cross-dataset generalization. Code is available at <https://github.com/giakoumoglou/distillers>.

1. Introduction

Knowledge distillation (KD) is a method where knowledge from a larger, well-trained model (the teacher) is transferred to a smaller, more efficient model (the student) by minimizing the Kullback-Leibler (KL) divergence between their outputs. This approach allows the student model to emulate the performance of the teacher model while maintaining reduced computational complexity, making it highly suitable for deployment in resource-constrained environments.

Representation learning is integral to KD as it enables the student model to learn meaningful feature representations that capture the underlying data distribution. Effective representation learning through KD can significantly enhance the performance of the student model across various tasks, including natural language processing, computer vision, and speech recognition [2, 22, 50].

Despite advancements in KD, efficiently transferring complex knowledge from the teacher to the student model remains a significant challenge. Traditional KD methods, which focus on aligning softmax outputs, often fail to capture the rich structural information embedded in the teacher’s intermediate representations. This limitation stems from the assumption that all dimensions are independent given the input, leading to a loss of relational information crucial for robust feature learning [47]. Recent approaches have attempted to address this issue through various means. For instance, attention transfer [54] and similarity-preserving KD [48] aim to align intermediate feature maps, while correlation congruence [39] focuses on preserving second-order feature statistics.

Contrastive Representation Distillation (CRD) [47] introduced the use of contrastive learning to maximize mutual information between teacher and student representations. CRD demonstrated that incorporating instance-level discrimination and a memory bank of negative samples could lead to more effective knowledge transfer. However, while CRD improved the preservation of structural information, it relies on a large memory buffer and does not explicitly enforce invariance in the learned representations.

Our proposed method, Invariant Consistency Distillation (ICD), builds upon the ideas of CRD while addressing its limitations. ICD introduces an explicit invariance penalty alongside contrastive learning, ensuring that the student’s representations are not only discriminative but also robust to variations in the input. Unlike CRD, ICD does not require a memory buffer, making it more memory-efficient. Furthermore, ICD employs a parameter-free approach with trainable components, including a dynamic temperature and bias for scaling and shifting logits. This allows for more flexible

arXiv:2407.11802v2 [cs.CV] 9 Sep 2024

and adaptive alignment between teacher and student representations without introducing additional hyperparameters. This combination enables ICD to capture a more comprehensive view of the teacher’s knowledge, including both instance-level discrimination and invariant features, leading to improved performance and generalization. Remarkably, in some cases, our objective allows the student model to surpass the teacher in terms of accuracy and robustness. We attribute this success to our objective’s ability to transfer all the information in the teacher’s representation, rather than just knowledge about independent output class probabilities, thereby enhancing representation learning.

Our contributions are threefold:

1. We introduce Invariant Consistency Distillation (ICD), a novel KD framework that combines contrastive learning with an explicit invariance penalty, ensuring consistent and robust representations between teacher and student models without the need for a memory buffer.
2. We demonstrate the effectiveness of ICD through extensive experiments on standard benchmarks, showing significant improvements in both accuracy and robustness. ICD outperforms other methods, achieving a 20.31% relative improvement¹ over the original KD. When combined with KD, it shows a 70.24% relative improvement over the original KD.
3. In some cases, we show that the student model can surpass the teacher model in terms of performance, highlighting the potential of our approach.

The rest of this paper is organized as follows. Section 2 reviews related work in KD and contrastive learning. Section 3 details our proposed ICD methodology. Section 4 presents our experimental setup and results, and Section 5 concludes the paper.

2. Related Work

Knowledge distillation. The seminal work on KD introduced the concept of transferring knowledge from large, cumbersome models to smaller, faster models while maintaining generalization power [22]. This method utilizes temperature scaling in the softmax outputs to better capture and transfer the knowledge of the teacher model. Various extensions and improvements to this approach have been proposed. For instance, using intermediate representations, or "hints", to guide the learning process has been suggested [41]. Another approach focuses on aligning the

attention maps of the teacher and student models to ensure they focus on similar regions during training [54]. Recent advancements include label decoupling [57], probability reweighting [35], and normalizing logits before applying softmax and KL divergence [46]. Some methods preserve relational knowledge between samples [48] and align correlation structures between teacher and student models [39]. Advanced architectures have been introduced, such as cross-stage connection paths [8], direct reuse of the teacher’s classifier [4], and many-to-one representation matching mechanisms [28]. Other learning approaches include differentiable meta-learning [13], contrastive intra-batch losses [7], and graph-based methods [31]. Some techniques focus on pairwise feature kernel comparisons [17], second-order gradient information [58], and self-regulated feature learning [29]. Notably, Contrastive Representation Distillation (CRD) [47] leverages contrastive learning to maximize mutual information between teacher and student representations. [14] proposes a training-free framework for architecture search in the context of KD.

Contrastive learning. Contrastive methods in self-supervised learning have proven effective for learning robust representations by maximizing mutual information. Techniques such as Contrastive Predictive Coding (CPC) [49], Deep InfoMax (DIM) [23], and Augmented Multiscale DIM (AMDIM) [3] use noise contrastive estimation (NCE) to create objectives that serve as bounds on mutual information. NCE converts the unsupervised learning problem into a classification problem, where the objective is to distinguish between true data samples (positives) and artificially generated noise samples (negatives). These approaches demonstrate that their objectives can maximize a lower bound on mutual information, which is crucial for learning meaningful representations. Recently, some methods have successfully combined contrastive learning with standard architectures, utilizing strong augmentations and memory banks to improve performance [9, 18]. Additionally, non-contrastive methods like BYOL [15] have emerged, achieving remarkable results without explicitly maximizing mutual information.

Our method, Invariant Consistency Distillation (ICD), bridges the gap between contrastive learning and KD by integrating contrastive learning principles with an explicit invariance penalty. Unlike methods that require large memory buffers [47], ICD employs a parameter-free approach with trainable components, including a dynamic temperature and bias for scaling and shifting logits. This allows for more flexible and adaptive alignment between teacher and student representations without introducing additional hyperparameters. By combining instance-level discrimination with an invariance constraint, ICD ensures that the student not only learns discriminative features but also preserves the overall structural knowledge of the teacher. Furthermore, our approach does not rely on fixed negative samples, instead using

¹Average relative improvement is calculated as: $\frac{1}{N} \sum_{i=1}^N \frac{\text{Acc}_{\text{ICD}}^i - \text{Acc}_{\text{KD}}^i}{\text{Acc}_{\text{KD}}^i - \text{Acc}_{\text{van}}^i}$, where $\text{Acc}_{\text{ICD}}^i$, Acc_{KD}^i , and $\text{Acc}_{\text{van}}^i$ represent the accuracies of ICD, KD, and vanilla training of the i -th student model, respectively [47].

a dynamic approach that adapts to the current state of the model during training.

3. Methodology

This section presents our methodology to improve the efficiency and accuracy of KD. Our method, Invariant Consistency Distillation (ICD), focuses on enhancing the alignment between the teacher and student models by ensuring that the representations learned by the student are consistent with those of the teacher.

3.1. Preliminaries

Problem setup. Let \mathcal{X} denote the available data and $\mathcal{Y} = \{Y_t\}_{t=1}^T$ be a set of unknown downstream tasks with Y_t representing the target for task t (e.g., classification, regression). In our KD framework, a high-capacity teacher neural network f^T imparts knowledge to a more compact student model f^S . A primary goal is not only to mimic the teacher’s performance with the student model but also to ensure that the student learns robust, generalizable representations from \mathcal{X} . These representations should transfer effectively to a wide range of tasks Y_t , extending beyond those explicitly modeled during training.

Formulation of knowledge distillation. Consider $x_i \in \mathcal{X}$, with $i = 1, 2, \dots, N$, as the input to these networks, typically an image. We represent the outputs at the penultimate layer (just before the final classification layer, or logits) as $z_i^T = f^T(x_i)$ and $z_i^S = f^S(x_i)$ for the teacher and student models, respectively. The primary objective of KD is to enable the student model to approximate the performance of the teacher model. The overall distillation process can be mathematically expressed as:

$$\mathcal{L} = \frac{1}{N} \sum_{i=1}^N [\mathcal{L}_{\text{sup}}(y_i, z_i^S) + \lambda \cdot \mathcal{L}_{\text{distill}}(z_i^T, z_i^S)] \quad (1)$$

where y_i represents the true label for the input x_i and λ is a hyperparameter that balances the supervised loss and the distillation loss. The supervised loss \mathcal{L}_{sup} is the task-specific alignment error between the network prediction and annotation. For image classification [10, 33, 40, 44], this is typically cross-entropy loss, while for object detection [6, 27], it includes bounding box regression. The distillation loss $\mathcal{L}_{\text{distill}}$ is the mimic error of the student network towards the teacher network, typically implemented as KL divergence between student and teacher outputs [22].

3.2. Theoretical Foundations

Invariant representation through causal inference. To leverage common assumptions and intuitions about data generation of the unknown downstream tasks Y_t , we start with the following assumptions: images $x_i \in \mathcal{X}$ are generated

from content and style variables; only content is relevant for the downstream tasks \mathcal{Y} ; content and style are independent, i.e., style changes are content-preserving. Let C and S be the latent variables describing content and style, respectively. In our causal model, C and S together generate the observed image x_i . Content C directly influences the task Y_t , while style S does not. Thus, content C has all the necessary information to predict Y_t . By assumption, content is a good representation of the data for downstream tasks and we therefore cast the goal of representation learning as estimating content. Using the principle of independent mechanisms [43], we conclude that under this causal model, interventions on S do not change the conditional distribution $\mathcal{P}(Y_t|C)$. Thus, $\mathcal{P}(Y_t|C)$ is invariant under changes in style S . We call C an invariant representation for Y_t under S , i.e.,

$$\mathcal{P}(Y_t|C)_{S=s_i} = \mathcal{P}(Y_t|C)_{S=s_j} \quad \forall s_i, s_j \in \mathcal{S}, \quad (2)$$

where $\mathcal{P}_{S=s}$ denotes the distribution arising from assigning S the value s , with \mathcal{S} the domain of S [38].

Invariance via model differences. Because the targets Y_t are not known, we create a proxy task Y^R to learn representations solely from the data \mathcal{X} . To transfer invariant representations from the teacher f^T to the student f^S , we aim to transfer content information while being invariant to style differences. The representations $f^S(\mathcal{X})$ and $f^T(\mathcal{X})$ must fulfill the following prediction invariant criteria:

$$\mathcal{P}(Y^R|f^S(\mathcal{X}))_{S=s_i} = \mathcal{P}(Y^R|f^T(\mathcal{X}))_{S=s_j} \quad (3)$$

However, C and S are latent and not directly accessible. We use the following insights to reformulate our objective:

- The teacher model f^T is assumed to have learned a good representation that captures content and is invariant to style.
- The difference between $f^T(\mathcal{X})$ and $f^S(\mathcal{X})$ can be attributed to style variations, as both models process the same input \mathcal{X} .

Based on these insights, we formulate our objective:

$$\mathbb{E}_{x_i} \left\{ \mathbb{E}_{s_i, s_j} \left[\sum_{s \in \{s_i, s_j\}} \mathcal{L}_s(Y^R, f^S(\mathcal{X}) - f^T(\mathcal{X})) \right] \right\} \quad (4)$$

subject to:

$$KL[\mathcal{P}(Y^R|f^T(\mathcal{X}))_{S=s_i}, \mathcal{P}(Y^R|f^S(\mathcal{X}))_{S=s_j}] \leq \rho \quad (5)$$

where s_i and s_j represent conceptual style interventions for the teacher and student models respectively, and \mathcal{L} is the

proxy task loss. This formulation allows us to model the potential differences in how the teacher and student models might interpret style information. The constraint ensures that the distributions of the proxy task predictions remain similar between the teacher and student, effectively transferring content information while allowing for style differences.

Contrastive instance discrimination for knowledge alignment. We extend the concept of instance discrimination using the principle of causal refinements [16]. For our proxy task, we assign each data point $x_i \in \mathcal{X}$ a unique identifier $y_i^R = i$, mirroring the instance discrimination approach prevalent in contrastive learning [9, 51]. We enforce similarity by making $f^S(x_i)$ similar to $f^T(x_i)$. We define:

$$\mathcal{P}(Y^R = j \mid f^S(x_i)) \propto \exp(\phi(f^S(x_i), f^T(x_i))/\tau), \quad (6)$$

where ϕ is a similarity function and τ is a temperature parameter for softmax.

Theoretical guarantee. Now, let Y^R be targets of a proxy task that is a refinement for all tasks in \mathcal{Y} . We show that if $f^T(\mathcal{X})$ is an invariant representation for Y^R , then $f^S(\mathcal{X})$ is also an invariant representation for tasks in \mathcal{Y} . This is summarized in the following theorem (see [34] for proof):

Theorem 1. Let $\mathcal{Y} = \{Y_t\}_{t=1}^T$ be a family of downstream tasks. Let Y^R be a refinement for all tasks in \mathcal{Y} . If $f^T(\mathcal{X})$ is an invariant representation for Y^R , then $f^S(\mathcal{X})$ is an invariant representation for all tasks in \mathcal{Y} , i.e.,

$$\begin{aligned} \mathcal{P}(Y^R \mid f^S(\mathcal{X}))_{s_i} &= \mathcal{P}(Y^R \mid f^T(\mathcal{X}))_{s_j} \Rightarrow \\ \mathcal{P}(Y_t \mid f^S(\mathcal{X}))_{s_i} &= \mathcal{P}(Y_t \mid f^T(\mathcal{X}))_{s_j} \end{aligned} \quad (7)$$

Thus, $f^S(\mathcal{X})$ is a representation that generalizes to \mathcal{Y} . This theorem states that if Y^R is a refinement of \mathcal{Y} , then learning a representation on Y^R is a sufficient condition for this representation to be useful on \mathcal{Y} . By integrating contrastive learning with an explicit invariance penalty, our approach ensures that the representations learned by the student model are consistent with those of the teacher model, leading to improved performance and robustness in KD.

3.3. Integrating Contrastive Learning and Invariance

We develop an objective function that introduces a structured approach to enforce this consistency between the teacher’s output z_i^T and the student’s output z_i^S . The objective combines contrastive learning with an explicit invariance penalty to ensure that the representations from both models are aligned. The objective function is formulated as:

$$\mathcal{L}_{\text{kd}}(z_i^T, z_i^S) = \mathcal{L}_{\text{contrast}}(z_i^T, z_i^S) + \alpha \cdot \mathcal{L}_{\text{invariance}}(z_i^T, z_i^S) \quad (8)$$

where α is a hyperparameter that balances the contrastive loss $\mathcal{L}_{\text{contrast}}$ and the invariance penalty $\mathcal{L}_{\text{invariance}}$.

The contrastive loss encourages the representations from the teacher and student models for the same input data to be similar, while simultaneously pushing apart representations from different data inputs:

$$\mathcal{L}_{\text{contrast}}(z_i^T, z_i^S) = -\log \frac{\exp(\phi(z_i^T, z_i^S)/\tau)}{\sum_{j=1}^M \exp(\phi(z_i^S, z_j^T)/\tau)} \quad (9)$$

where ϕ is a similarity function, τ is a temperature parameter, and M is the number of negative samples. In our framework, positives are obtained by pairing the outputs z_i^T and z_i^S from the teacher and student models for the same input instance. Negatives are sampled from other instances within the mini batch, following the instance discrimination principle to differentiate between distinct data points [9, 51]. The similarity function ϕ is chosen as the cosine similarity:

$$\phi(z_i^T, z_i^S) = \frac{z_i^T \cdot z_i^S}{\|z_i^T\| \|z_i^S\|} \quad (10)$$

To enforce invariance, we minimize the discrepancy between the distributions of representations z_i^T and z_i^S . This penalty ensures that the student model learns to produce representations that are invariant to the teacher model’s transformations:

$$\mathcal{L}_{\text{invariance}}(z_i^T, z_i^S) = KL(p(z_i^T) \parallel p(z_i^S)) \quad (11)$$

where KL denotes the KL divergence between the distributions $p(z_i^T)$ and $p(z_i^S)$, ensuring that the student model’s outputs faithfully replicate the teacher model’s transformations across different inputs.

The combination of contrastive loss and invariance penalty ensures that the learned representations are both discriminative and robust to style variations. This is formalized by the following theorem:

Theorem 2. Let f be a representation function learned by minimizing \mathcal{L}_{kd} . Under the assumption that f is L-Lipschitz and that the data is sub-Gaussian, the expected loss satisfies:

$$\mathbb{E}[\mathcal{L}_{\text{kd}}] \leq \mathcal{O}\left(\frac{1}{\sqrt{N}} + \alpha \cdot \frac{\log M}{M}\right) \quad (12)$$

This theorem guarantees that as the number of samples N and the number of negative samples M increases, the loss converges to zero, ensuring both high-quality representations and invariance.

In practice, we implement the objective using mini-batch stochastic gradient descent. The representations z_i^T and z_i^S are obtained from the last layer of the teacher and student models, respectively. We further encode z_i^T and z_i^S using a projection head to match the dimensions. The projection head is trained using stochastic gradient descent as well.

This ensures that the representations from both models are compatible for comparison and alignment. Additionally, we normalize the outputs z_i^T and z_i^S before computing the loss, ensuring that the representations lie on a unit hypersphere. This ensures that the representations from both models are compatible for comparison and alignment.

Instead of using a large memory buffer as in CRD [47], we use a trainable temperature parameter τ and a bias b to scale and shift the logits. Specifically, we compute the logits as the matrix multiplication of the student and teacher features, scaled by the exponential of the learnable temperature parameter τ and adjusted by the learnable bias b . The temperature parameter τ is clamped to a maximum value to ensure stability, and the bias b adjusts the logits dynamically. This approach allows for greater flexibility and adaptability in the alignment of the teacher and student representations, thereby improving the performance and consistency of the KD process.

The final objective function, which includes the supervised loss and standard KL divergence, is given by:

$$\mathcal{L} = \frac{1}{N} \sum_{i=1}^N [\mathcal{L}_{\text{sup}}(y_i, z_i^S) + \lambda \cdot \mathcal{L}_{\text{distill}}(z_i^T, z_i^S) + \beta \cdot \mathcal{L}_{\text{kd}}(z_i^T, z_i^S)] \quad (13)$$

where β is a hyperparameter that balances \mathcal{L}_{kd} .

4. Experiments

We evaluate our ICD framework in the KD task for model compression of a large network to a smaller one, similar to [1, 21, 22, 24, 25, 36, 37, 39, 41, 47, 48, 53, 54]. This method aligns with common practices in the field, ensuring a fair comparison between different techniques.

Datasets. (1) CIFAR-100 [26] contains 50,000 training images with 500 images per class and 10,000 test images. (2) ImageNet ILSVRC-2012 [12] includes 1.2 million images from 1,000 classes for training and 50,000 for validation. (3) STL-10 [11] consists of a training set of 5,000 labeled images from 10 classes and 100,000 unlabeled images, and a test set of 8,000 images. (4) Tiny ImageNet (TIN-200) [12] comprises 200 classes, each with 500 training images and 50 validation images.

Setup. We experiment with student-teacher combinations of different capacities, such as ResNet [19] or Wide ResNet (WRN) [55], VGG [45], MobileNet [42], and ShuffleNet [30, 56] (more details are described in the supplementary material). The only hyperparameters in our method are: the loss coefficient β , which balances the ICD loss with other loss terms and the internal loss coefficient α , which balances the contrastive and invariance losses within the ICD loss. We set $\alpha = 0.5$ and $\beta = 1$ and ablate both α and β in Section 4.5. The hyperparameter λ is set to 1.0 for the KL divergence loss to maintain consistency with [4, 5, 47]. Both the student

and teacher outputs are projected to a 128-dimensional space using a projection head consisting of a single linear layer, followed by ℓ_2 normalization. We train for a total of 240 epochs. More details on the training procedures can be found in the supplementary material.

Comparison. We compare our approach to the following state-of-the-art methods: (1) KD [22]; (2) FitNets [41]; (3) AT [54]; (4) SP [48]; (5) CC [39]; (6) VID [1]; (7) RKD [36]; (8) PKT [37]; (9) AB [21]; (10) FT [25]; (11) FSP [53]; (12) NST [24]; (13) CRD [47]; (14) OFD [20]; (15) WSLD [57]; (16) IPWD [35]. In the supplementary material, we include additional methods: (17) SRRL [52]; (18) SemCKD [5]; (19) ReviewKD [8]; (20) SimKD [4]; (21) DistPro [13]; (22) NORM [28]; (23) ITRD [32]; (24) FKD [17]; (25) CRCD [58]; (26) EGA [31]; (27) WCoRD [7].

4.1. Results on CIFAR-100

Table 1 and Table 2 provide a comprehensive comparison of top-1 accuracies across various KD methods for both identical and differing architectures between student and teacher models on the CIFAR-100 dataset. Specifically, Table 1 focuses on scenarios where the student and teacher share the same architecture, while Table 2 explores settings with differing architectures. Our proposed method, ICD, and its combination with KD, consistently achieve superior performance compared to other distillation objectives, including the original KD. Our method surpasses the teacher network’s performance in both same-architecture (WRN-40-2 to WRN-16-2) and cross-architecture (WRN-40-2 to ShuffleNet-v1) scenarios, achieving accuracy gains of 0.45% and 0.90%, respectively. While CRD and CRD combined with KD also show competitive results, especially in some architecture configurations, ICD and ICD combined with KD frequently show higher accuracies. Both CRD and ICD leverage contrastive learning objectives, which promote better alignment between student and teacher models.

4.2. Results on ImageNet

Table 3 showcases the top-1 accuracy of student networks that were trained using various distillation methods on ImageNet. The results demonstrate the effectiveness of our method on large-scale datasets, highlighting its ability to distill knowledge from complex models and enhance the performance of student networks. Our approach achieves competitive results, surpassing KD and attaining state-of-the-art performance in ResNet-50 to ResNet-18 distillation. Our approach also shows improvement across different architectures, demonstrating its effectiveness in various distillation scenarios.

4.3. Capturing Inter-class Correlations

Cross-entropy loss ignores the correlations among class logits in a teacher network, often leading to suboptimal

Teacher	WRN-40-2	WRN-40-2	resnet-56	resnet-110	resnet-110	resnet-32x4	VGG-13
Student	WRN-16-2	WRN-40-1	resnet-20	resnet-20	resnet-32	resnet-8x4	VGG-8
Teacher	75.61	75.61	72.34	74.31	74.31	79.42	74.64
Student	73.26	71.98	69.06	69.06	71.14	72.50	70.36
KD [22]	74.92	73.54	70.66	70.67	73.08	73.33	72.98
FitNet [41]	73.58 (↓)	72.24 (↓)	69.21 (↓)	68.99 (↓)	71.06 (↓)	73.50 (↓)	71.02 (↓)
AT [54]	74.08 (↓)	72.77 (↓)	70.55 (↓)	70.22 (↓)	72.31 (↓)	73.44 (↓)	71.43 (↓)
SP [48]	73.83 (↓)	72.43 (↓)	69.67 (↓)	70.04 (↓)	72.69 (↓)	72.94 (↓)	72.68 (↓)
CC [39]	73.56 (↓)	72.21 (↓)	69.63 (↓)	69.48 (↓)	71.48 (↓)	72.97 (↓)	70.81 (↓)
VID [1]	74.11 (↓)	73.30 (↓)	70.38 (↓)	70.16 (↓)	72.61 (↓)	73.09 (↓)	71.23 (↓)
RKD [36]	73.35 (↓)	72.22 (↓)	69.61 (↓)	69.25 (↓)	71.82 (↓)	71.90 (↓)	71.48 (↓)
PKT [37]	74.54 (↓)	73.45 (↓)	70.34 (↓)	70.25 (↓)	72.61 (↓)	73.64 (↑)	72.88 (↓)
AB [21]	72.50 (↓)	72.38 (↓)	69.47 (↓)	69.53 (↓)	70.98 (↓)	73.17 (↓)	70.94 (↓)
FT [25]	73.25 (↓)	71.59 (↓)	69.84 (↓)	70.22 (↓)	72.37 (↓)	72.86 (↓)	70.58 (↓)
FSP [53]	72.91 (↓)	n/a	69.95 (↓)	70.11 (↓)	71.89 (↓)	72.62 (↓)	70.33 (↓)
NST [24]	73.68 (↓)	72.24 (↓)	69.60 (↓)	69.53 (↓)	71.96 (↓)	73.30 (↓)	71.53 (↓)
CRD [47]	75.48 (↑)	74.14 (↑)	71.16 (↑)	71.46 (↑)	73.48 (↑)	<u>75.51</u> (↑)	73.94 (↑)
CRD+KD [47]	<u>75.64</u> (↑)	74.38 (↑)	<u>71.63</u> (↑)	<u>71.56</u> (↑)	73.75 (↑)	75.46 (↑)	74.29 (↑)
OFD [20]	75.24 (↑)	74.33 (↑)	70.38 (↑)	n/a	73.23 (↑)	74.95 (↑)	<u>73.95</u> (↑)
WSLD [57]	n/a	<u>73.74</u> (↑)	71.53 (↑)	n/a	73.36 (↑)	74.79 (↑)	n/a
IPWD [35]	n/a	74.64 (↑)	71.32 (↑)	n/a	73.91 (↑)	76.03 (↑)	n/a
ICD (ours)	74.99 (↑)	73.69 (↑)	71.18 (↑)	71.00 (↑)	73.12 (↑)	74.23 (↑)	73.22 (↑)
ICD+KD (ours)	76.06 (↑)	74.76 (↑)	71.81 (↑)	72.03 (↑)	<u>73.62</u> (↑)	75.09 (↑)	<u>73.95</u> (↑)

Table 1. Test top-1 accuracy (%) of student networks on CIFAR-100, comparing students and teachers of the same architecture using various distillation methods. ↑ denotes outperformance over KD and ↓ denotes underperformance. The values in bold indicate the maximum of each column while underlined values mark the second best.

Teacher	VGG-13	ResNet-50	ResNet-50	ResNet-32x4	ResNet-32x4	WRN-40-2
Student	MobileNet-v2	MobileNet-v2	VGG-8	ShuffleNet-v1	ShuffleNet-v2	ShuffleNet-v1
Teacher	74.64	79.34	79.34	79.42	79.42	75.61
Student	64.6	64.6	70.36	70.5	71.82	70.5
KD [22]	67.37	67.35	73.81	74.07	74.45	74.83
FitNet [41]	64.14 (↓)	63.16 (↓)	70.69 (↓)	73.59 (↓)	73.54 (↓)	73.73 (↓)
AT [54]	59.40 (↓)	58.58 (↓)	71.84 (↓)	71.73 (↓)	72.73 (↓)	73.32 (↓)
SP [48]	66.30 (↓)	68.08 (↓)	73.34 (↓)	73.48 (↓)	74.56 (↑)	74.52 (↓)
CC [39]	64.86 (↓)	65.43 (↓)	70.25 (↓)	71.14 (↓)	71.29 (↓)	71.38 (↓)
VID [1]	65.56 (↓)	67.57 (↓)	70.30 (↓)	73.38 (↓)	73.40 (↓)	73.61 (↓)
RKD [36]	64.52 (↓)	64.43 (↓)	71.50 (↓)	72.28 (↓)	73.21 (↓)	72.21 (↓)
PKT [37]	67.13 (↓)	66.52 (↓)	73.01 (↓)	74.10 (↑)	74.69 (↑)	73.89 (↓)
AB [21]	66.06 (↓)	67.20 (↓)	70.65 (↓)	73.55 (↓)	74.31 (↓)	73.34 (↓)
FT [25]	61.78 (↓)	60.99 (↓)	70.29 (↓)	71.75 (↓)	72.50 (↓)	72.03 (↓)
NST [24]	58.16 (↓)	64.96 (↓)	71.28 (↓)	74.12 (↑)	74.68 (↑)	76.09 (↑)
CRD [47]	<u>69.73</u> (↑)	69.11 (↑)	74.30 (↑)	75.11 (↑)	75.65 (↑)	76.05 (↑)
CRD+KD [47]	69.94 (↑)	69.54 (↑)	<u>74.58</u> (↑)	75.12 (↑)	76.05 (↑)	76.27 (↑)
OFD [20]	69.48 (↑)	69.04 (↑)	n/a	<u>75.98</u> (↑)	76.82 (↑)	75.85 (↑)
WSLD [57]	n/a	68.79 (↑)	73.80 (↑)	75.09 (↑)	n/a	75.23 (↑)
IPWD [35]	n/a	70.25 (↑)	74.97 (↑)	76.03 (↑)	n/a	<u>76.44</u> (↑)
ICD (ours)	68.35 (↑)	67.39 (↑)	73.85 (↑)	74.26 (↑)	75.26 (↑)	74.98 (↑)
ICD+KD (ours)	69.55 (↑)	<u>69.91</u> (↑)	74.08 (↑)	75.27 (↑)	<u>76.58</u> (↑)	76.51 (↑)

Table 2. Test top-1 accuracy (%) of student networks on CIFAR-100 involving students and teachers from different architectures, using various distillation methods. ↑ denotes outperformance over KD and ↓ denotes underperformance. The values in bold indicate the maximum of each column while underlined values mark the second best.

Teacher	ResNet-34	ResNet-50	ResNet-50
Student	ResNet-18	ResNet-18	MobileNet
Teacher	73.31	76.16	76.16
Student	69.75	69.75	69.63
KD [22]	70.67	71.29	70.49
AT [54]	71.03 (↑)	71.18 (↓)	70.18 (↓)
SP [48]	70.62 (↑)	71.08 (↓)	n/a
CC [39]	69.96 (↓)	n/a	n/a
VID [1]	n/a	71.11 (↓)	n/a
RKD [36]	70.40 (↓)	n/a	68.50 (↓)
AB [21]	n/a	n/a	68.89 (↓)
FT [25]	n/a	n/a	69.88 (↓)
FSP [53]	70.58 (↓)	n/a	n/a
NST [24]	70.29 (↓)	n/a	n/a
CRD [47]	71.17 (↑)	<u>71.25</u> (↓)	69.07 (↓)
OFD [20]	71.03 (↑)	n/a	71.33 (↑)
WSLD [57]	72.04 (↑)	n/a	71.52 (↑)
IPWD [35]	<u>71.88</u> (↑)	n/a	72.65 (↑)
ICD (ours)	71.10 (↑)	71.38 (↑)	70.51 (↑)
ICD+KD (ours)	71.71 (↑)	71.65 (↑)	<u>71.55</u> (↑)

Table 3. Test top-1 (%) on ImageNet validation test using various distillation methods. The table compares students and teachers of the same and different architecture. ↑ denotes outperformance over KD and ↓ denotes underperformance. The values in bold indicate the maximum of each column while underlined values mark the second best.

knowledge transfer. By employing "soft targets", distillation methods such as those described by [22] have successfully captured these correlations, enhancing student learning. Figure 1 evaluates the effectiveness of various distillation approaches on the CIFAR-100 KD task using WRN-40-2 as the teacher and WRN-40-1 as the student. Specifically, we compare students trained without distillation, with attention transfer [54], with KL divergence [22], and with our proposed ICD method. Our results demonstrate that ICD achieves close correlation alignment between teacher and student logits, as evidenced by the minimal differences in their correlation matrices. However, compared to CRD [47], our method achieves less optimal matching, though it still significantly enhances learning efficiency and lowers error rates. The smaller discrepancies between teacher and student logits clearly indicate that the ICD objective captures a substantial amount of correlation structure in the logit, resulting in lower error rates, although it is surpassed slightly by CRD in achieving the closest match. Moreover, our method also enhances representation learning as it employs a contrastive objective.

4.4. Transferability of Representations

Our research focuses on transferring knowledge from a teacher network to a student network while learning repre-

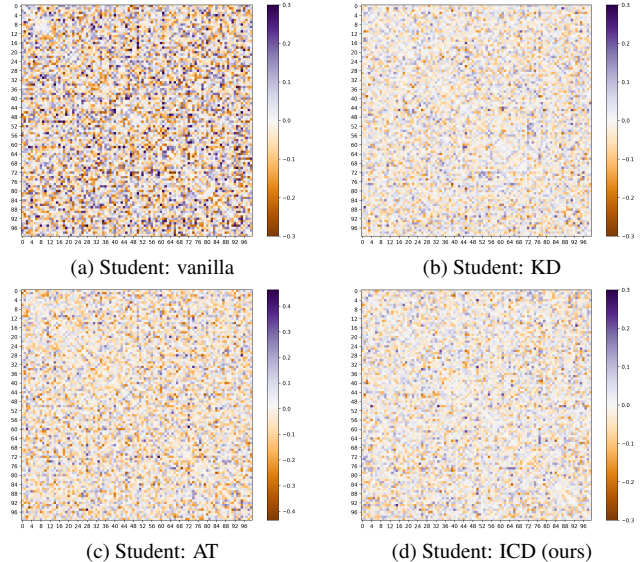


Figure 1. Comparison of correlation matrix differences between teacher and student logits across various distillation methods on the CIFAR-100 task. Subfigures show results for (a) students trained without distillation, (b) with attention transfer [54], (c) with KL divergence [22], and (d) with our ICD method, highlighting better matching between student’s and teacher’s correlations. Results have been re-implemented according to [47].

sentations that embody general knowledge applicable across various tasks and datasets. To investigate this, we employ a distillation process where a WRN-40-2 teacher network transfers its learned representations to a WRN-16-2 student network, which can either be trained directly from the CIFAR-100 dataset or through distillation. In our experiments, the student network functions as a fixed feature extractor, processing images from STL-10 and TIN-200, both resized to 32×32 . To assess the generalizability of these representations, we train a linear classifier on top of the last feature layer to perform 10-way classification for STL-10 and 200-way classification for TIN-200. The effectiveness of different distillation methods in enhancing the transferability of these representations is detailed in Table 4. Our results indicate that the ICD method, both standalone and in combination with KD, significantly outperforms all other distillation methods in enhancing the transferability of learned representations across different datasets. This superior transferability suggests that ICD encourages the student to learn more general and robust features, which are less overfitted to the specific training dataset and more applicable to diverse visual recognition tasks.

4.5. Ablation Study

There are three main hyperparameters in our objective: the internal ICD coefficient α , which balances the contrastive

	Teacher	Student	KD	AT	FitNet	CRD	CRD+KD	ICD	ICD+KD
CIFAR-100→STL-10	68.6	69.7	70.9	70.7	70.3	71.6	72.2	71.2	72.5
CIFAR-100→TIN-200	31.5	33.7	33.9	34.2	33.5	35.6	35.5	35.0	36.2

Table 4. Test top-1 accuracy (%) of WRN-16-2 (student) distilled from WRN-40-2 (teacher). In this setup, the representations learned from the CIFAR-100 dataset are transferred to the STL-10 and TIN-200 datasets. The network is frozen, and a linear classifier is trained on the last feature layer to perform classification with 10 classes (STL-10) or 200 classes (TIN-200). The values in bold indicate the maximum of each row.

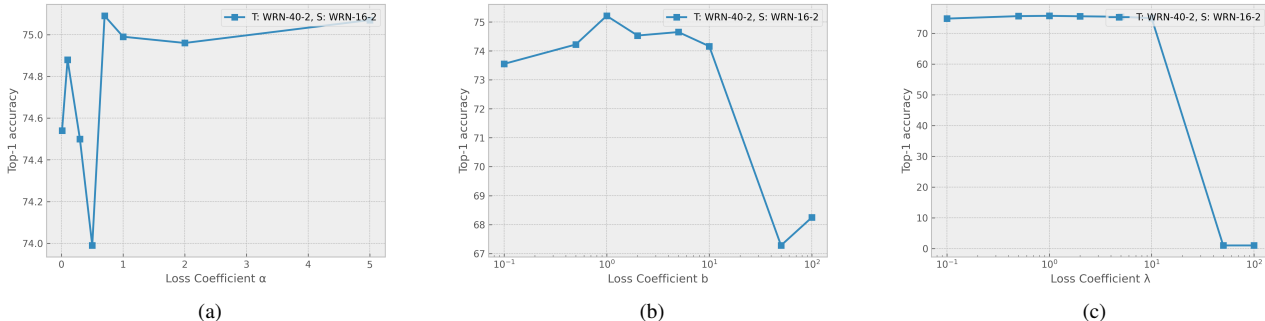


Figure 2. Ablation study results on CIFAR-100 using WRN-40-2 as the teacher and WRN-16-2 as the student. (a) Effect of the internal ICD coefficient α on performance. (b) Effect of ICD loss coefficient β on performance (logarithmic scale). (c) Effect of loss coefficient λ on performance.

and invariance losses within the ICD loss; the ICD loss coefficient β , which balances the ICD loss with other loss terms; and the loss coefficient λ , which is typically set to 1.0 but can be adjusted to affect the weighting of certain components. We conduct an ablation study to analyze the impact of these hyperparameters. For this study, we adopt WRN-40-2 as the teacher and WRN-16-2 as the student. Experiments are conducted on CIFAR-100, and the results are shown in Figure 2.

Internal loss coefficient α . We tested different values for α : 0.01, 0.1, 0.3, 0.5, 0.7, 1, 2, and 5. As shown in Figure 2a, very low α values degrade performance, while increasing α beyond 1 slightly reduces performance. This suggests that a balanced contribution from both the contrastive and invariance components of the ICD loss is crucial for optimal KD.

Loss coefficient β . We varied β from 0.1 to 100, considering values of 0.1, 0.5, 1, 2, 5, 10, 50, and 100. As illustrated in Figure 2b, extremely high β values cause significant degradation in performance due to the overwhelming contribution of the ICD loss compared to other loss terms. Very low values of β also lead to decreased performance. The optimal range for β is between 0.5 and 10, suggesting that the ICD loss should be weighted similarly to other loss terms for the best results.

Loss coefficient λ . While λ is typically set to 1.0 [4,5,47], we tested values from 0.1 to 100. As shown in Figure 2c,

high values (i.e., $\lambda = 50$ and 100) lead to collapsing training. Lower values, such as 0.5 to 1.0, have similar performance.

5. Conclusions

We have developed a new technique for neural network distillation that leverages invariant consistency to improve the traditional KD process. Our method, demonstrated for model compression, can also be applied to cross-modal knowledge transfer and ensemble distillation from a group of teachers to a single student network. It combines contrastive learning with an invariance penalty to better align teacher and student models. Unlike CRD [47], our approach requires no memory bank. Instead, it uses a trainable temperature parameter and a bias to scale and shift the logits. By leveraging the contrastive nature, ICD not only aligns the student with the teacher’s output but also improves the quality of the learned embeddings, leading to better generalization and performance. Our experiments demonstrate that this approach consistently outperforms standard KD methods, enhancing both accuracy and robustness. Notably, our method has shown excellent performance on CIFAR-100 and ImageNet and has been successfully applied to other datasets such as TIN-200 and STL-10. In some cases, student models using our KD technique even exceeded the performance of their teacher models, suggesting significant potential for this approach in optimizing neural network training and deployment in various settings.

References

- [1] Sungsoo Ahn, Shell Xu Hu, Andreas Damianou, Neil D Lawrence, and Zhenwen Dai. Variational information distillation for knowledge transfer. In *Proceedings of the IEEE Conference on Computer Vision and Pattern Recognition*, pages 9163–9171, 2019. 5, 6, 7
- [2] Yusuf Aytar, Carl Vondrick, and Antonio Torralba. Soundnet: Learning sound representations from unlabeled video. In *Advances in Neural Information Processing Systems*, pages 892–900, 2016. 1
- [3] Philip Bachman, R Devon Hjelm, and William Buchwalter. Learning representations by maximizing mutual information across views, 2019. 2
- [4] Defang Chen, Jian-Ping Mei, Hailin Zhang, Can Wang, Yan Feng, and Chun Chen. Knowledge distillation with the reused teacher classifier, 2022. 2, 5, 8
- [5] Defang Chen, Jian-Ping Mei, Yuan Zhang, Can Wang, Yan Feng, and Chun Chen. Cross-layer distillation with semantic calibration, 2021. 5, 8
- [6] Gongfan Chen, Yuting Wang, Jiajun Xu, Zhe Du, Qionghai Dai, Shiyang Geng, and Tao Mei. Learning efficient object detection models with knowledge distillation. In *Advances in Neural Information Processing Systems*, pages 742–751, 2017. 3
- [7] Liqun Chen, Dong Wang, Zhe Gan, Jingjing Liu, Ricardo Henao, and Lawrence Carin. Wasserstein contrastive representation distillation, 2021. 2, 5
- [8] Pengguang Chen, Shu Liu, Hengshuang Zhao, and Jiaya Jia. Distilling knowledge via knowledge review, 2021. 2, 5
- [9] Ting Chen, Simon Kornblith, Mohammad Norouzi, and Geoffrey Hinton. A simple framework for contrastive learning of visual representations, 2020. 2, 4
- [10] Jang Hyun Cho and Bharath Hariharan. On the efficacy of knowledge distillation. In *Proceedings of the IEEE/CVF International Conference on Computer Vision*, pages 4794–4802, 2019. 3
- [11] Adam Coates and Andrew Y. Ng. The importance of encoding versus training with sparse coding and vector quantization. In *Proceedings of the 28th International Conference on International Conference on Machine Learning, ICML’11*, page 921–928, Madison, WI, USA, 2011. Omnipress. 5
- [12] Jia Deng, Wei Dong, Richard Socher, Li-Jia Li, K. Li, and Li Fei-Fei. Imagenet: A large-scale hierarchical image database. *2009 IEEE Conference on Computer Vision and Pattern Recognition*, pages 248–255, 2009. 5
- [13] Xueqing Deng, Dawei Sun, Shawn Newsam, and Peng Wang. Distpro: Searching a fast knowledge distillation process via meta optimization, 2022. 2, 5
- [14] Peijie Dong, Lujun Li, and Zimian Wei. Diswot: Student architecture search for distillation without training, 2023. 2
- [15] Jean-Bastien Grill, Florian Strub, Florent Althé, Corentin Tallec, Pierre H. Richemond, Elena Buchatskaya, Carl Doersch, Bernardo Avila Pires, Zhaohan Daniel Guo, Mohammad Gheshlaghi Azar, Bilal Piot, Koray Kavukcuoglu, Rémi Munos, and Michal Valko. Bootstrap your own latent: A new approach to self-supervised learning, 2020. 2
- [16] R. Hadsell, S. Chopra, and Y. LeCun. Dimensionality reduction by learning an invariant mapping. In *2006 IEEE Computer Society Conference on Computer Vision and Pattern Recognition - Volume 2 (CVPR’06)*, volume 2, page 1735–1742. IEEE. 4
- [17] Bobby He and Mete Ozay. Feature kernel distillation. In *International Conference on Learning Representations*, 2022. 2, 5
- [18] Kaiming He, Haoqi Fan, Yuxin Wu, Saining Xie, and Ross Girshick. Momentum contrast for unsupervised visual representation learning, 2020. 2
- [19] Kaiming He, Xiangyu Zhang, Shaoqing Ren, and Jian Sun. Deep residual learning for image recognition, 2015. 5
- [20] Byeongho Heo, Jeesoo Kim, Sangdoo Yun, Hyojin Park, Nojun Kwak, and Jin Young Choi. A comprehensive overhaul of feature distillation, 2019. 5, 6, 7
- [21] Byeongho Heo, Minsik Lee, Seong Joon Yun, Jin Young Choi, and In So Kweon. Knowledge transfer via distillation of activation boundaries formed by hidden neurons. In *Proceedings of the AAAI Conference on Artificial Intelligence*, pages 3779–3787, 2019. 5, 6, 7
- [22] Geoffrey Hinton, Oriol Vinyals, and Jeff Dean. Distilling the knowledge in a neural network, 2015. 1, 2, 3, 5, 6, 7
- [23] R Devon Hjelm, Alex Fedorov, Samuel Lavoie-Marchildon, Karan Grewal, Phil Bachman, Adam Trischler, and Yoshua Bengio. Learning deep representations by mutual information estimation and maximization, 2019. 2
- [24] Zehao Huang and Naiyan Wang. Like what you like: Knowledge distill via neuron selectivity transfer. In *Advances in Neural Information Processing Systems*, pages 185–195, 2017. 5, 6, 7
- [25] Jangho Kim, Seongwon Park, and Nojun Kwak. Paraphrasing complex network: Network compression via factor transfer. In *Advances in Neural Information Processing Systems*, pages 2760–2769, 2018. 5, 6, 7
- [26] Alex Krizhevsky. Learning multiple layers of features from tiny images. pages 32–33, 2009. 5
- [27] Wei Liu, Andrew Rabinovich, and Alexander C Berg. Learning efficient single-stage pedestrian detectors by asymptotic localization fitting. In *Proceedings of the European Conference on Computer Vision (ECCV)*, pages 618–634, 2018. 3
- [28] Xiaolong Liu, Lujun Li, Chao Li, and Anbang Yao. Norm: Knowledge distillation via n-to-one representation matching, 2023. 2, 5
- [29] Li Lujun. Self-regulated feature learning via teacher-free feature distillation. In *European Conference on Computer Vision (ECCV)*, 2022. 2
- [30] Ningning Ma, Xiangyu Zhang, Hai-Tao Zheng, and Jian Sun. Shufflenet v2: Practical guidelines for efficient cnn architecture design. In *Proceedings of the European Conference on Computer Vision (ECCV)*, pages 116–131, 2018. 5
- [31] Yuchen Ma, Yanbei Chen, and Zeynep Akata. Distilling knowledge from self-supervised teacher by embedding graph alignment, 2022. 2, 5
- [32] Roy Miles, Adrian Lopez Rodriguez, and Krystian Mikolajczyk. Information theoretic representation distillation, 2022. 5

- [33] Arun Mishra and Debbie Marr. Apprentice: Using knowledge distillation techniques to improve low-precision network accuracy. In *International Conference on Learning Representations*, 2017. 3
- [34] Jovana Mitrovic, Brian McWilliams, Jacob Walker, Lars Buesing, and Charles Blundell. Representation learning via invariant causal mechanisms, 2020. 4
- [35] Yulei Niu, Long Chen, Chang Zhou, and Hanwang Zhang. Respecting transfer gap in knowledge distillation, 2022. 2, 5, 6, 7
- [36] Wonpyo Park, Dongju Kim, Yan Lu, and Minsu Cho. Relational knowledge distillation. In *Proceedings of the IEEE Conference on Computer Vision and Pattern Recognition*, pages 3967–3976, 2019. 5, 6, 7
- [37] Nikolaos Passalis and Anastasios Tefas. Learning deep representations with probabilistic knowledge transfer. In *Proceedings of the European Conference on Computer Vision (ECCV)*, pages 268–284, 2018. 5, 6
- [38] Judea Pearl. *Causality: Models, Reasoning, and Inference*. Cambridge University Press, Sept. 2009. 3
- [39] Baoyun Peng, Xi Li, Yifan Wu, Yizhou Fan, Bo Wang, Qi Tian, and Jun Liang. Correlation congruence for knowledge distillation. In *Proceedings of the IEEE International Conference on Computer Vision*, pages 5007–5016, 2019. 1, 2, 5, 6, 7
- [40] Antonio Polino, Razvan Pascanu, and Dan Alistarh. Model compression via distillation and quantization. In *International Conference on Learning Representations*, 2018. 3
- [41] Adriana Romero, Nicolas Ballas, Samira Ebrahimi Kahou, Antoine Chassang, Carlo Gatta, and Yoshua Bengio. Fitnets: Hints for thin deep nets. In *Proceedings of the 4th International Conference on Learning Representations*, 2014. 2, 5, 6
- [42] Mark Sandler, Andrew Howard, Menglong Zhu, Andrey Zhmoginov, and Liang-Chieh Chen. Mobilenetv2: Inverted residuals and linear bottlenecks. In *Proceedings of the IEEE conference on computer vision and pattern recognition*, pages 4510–4520, 2018. 5
- [43] Bernhard Scholkopf, Jonas Peters, and Dominik Janzing. *Elements of causal inference*. Adaptive Computation and Machine Learning series. MIT Press, London, England, Nov. 2017. 3
- [44] Li Shen and Marios Savvides. Amalgamating knowledge towards comprehensive classification. In *Proceedings of the IEEE/CVF Conference on Computer Vision and Pattern Recognition*, pages 1687–1696, 2020. 3
- [45] Karen Simonyan and Andrew Zisserman. Very deep convolutional networks for large-scale image recognition, 2015. 5
- [46] Shangquan Sun, Wenqi Ren, Jingzhi Li, Rui Wang, and Xiaochun Cao. Logit standardization in knowledge distillation, 2024. 2
- [47] Yonglong Tian, Dilip Krishnan, and Phillip Isola. Contrastive representation distillation, 2022. 1, 2, 5, 6, 7, 8
- [48] Frederick Tung and Greg Mori. Similarity-preserving knowledge distillation. In *Proceedings of the IEEE International Conference on Computer Vision*, pages 1365–1374, 2019. 1, 2, 5, 6, 7
- [49] Aaron van den Oord, Yazhe Li, and Oriol Vinyals. Representation learning with contrastive predictive coding, 2019. 2
- [50] Lin Wang and Kuk-Jin Yoon. Knowledge distillation and student-teacher learning for visual intelligence: A review and new outlooks. *IEEE Transactions on Pattern Analysis and Machine Intelligence*, 44(6):3048–3068, 2022. 1
- [51] Zhirong Wu, Yuanjun Xiong, Stella Yu, and Dahua Lin. Unsupervised feature learning via non-parametric instance-level discrimination, 2018. 4
- [52] Jing Yang, Brais Martinez, Adrian Bulat, and Georgios Tzimiropoulos. Knowledge distillation via softmax regression representation learning. In *International Conference on Learning Representations*, 2021. 5
- [53] Junho Yim, Donggyu Joo, Jihoon Bae, and Junmo Kim. A gift from knowledge distillation: Fast optimization, network minimization and transfer learning. In *Proceedings of the IEEE Conference on Computer Vision and Pattern Recognition*, pages 4133–4141, 2017. 5, 6, 7
- [54] Sergey Zagoruyko and Nikos Komodakis. Paying more attention to attention: Improving the performance of convolutional neural networks via attention transfer. In *Proceedings of the 5th International Conference on Learning Representations*, 2016. 1, 2, 5, 6, 7
- [55] Sergey Zagoruyko and Nikos Komodakis. Wide residual networks, 2017. 5
- [56] Xiangyu Zhang, Xinyu Zhou, Mengxiao Lin, and Jian Sun. Shufflenet: An extremely efficient convolutional neural network for mobile devices. In *Proceedings of the IEEE conference on computer vision and pattern recognition*, pages 6848–6856, 2018. 5
- [57] Helong Zhou, Liangchen Song, Jiajie Chen, Ye Zhou, Guoli Wang, Junsong Yuan, and Qian Zhang. Rethinking soft labels for knowledge distillation: A bias-variance tradeoff perspective, 2021. 2, 5, 6, 7
- [58] Jinguo Zhu, Shixiang Tang, Dapeng Chen, Shijie Yu, Yakun Liu, Aijun Yang, Mingzhe Rong, and Xiaohua Wang. Complementary relation contrastive distillation, 2021. 2, 5